Geostrophic Circulation in a Rectangular Basin with a Circumpolar Connection

R. M. SAMELSON

College of Oceanic and Atmospheric Sciences, Oregon State University, Corvallis, Oregon

8 January 1999 and 19 July 1999

ABSTRACT

A simple theory is presented for steady geostrophic circulation of a stratified fluid in a rectangular basin with a circumpolar connection. The interior flow obeys the β-plane Sverdrup vorticity balance, and the circulation is closed by geostrophic boundary currents. The circulation is forced by surface thermal gradients and wind-driven Ekman transport near the latitudes of the circumpolar connection. A thermal circumpolar current arises in response to imposed surface thermal gradients and northward Ekman transport across the gap latitudes. The transport of this model circumpolar current depends on the imposed surface thermal gradients and the gap geometry, but not on the strength of the wind forcing. In contrast, the circulation induced in a related reduced-gravity model by Sverdrup transport into the gap latitudes has zero zonally integrated zonal transport. The thermal current arises as a consequence of the geostrophic constraint, which requires that the northern region fill with warm fluid until it reaches the sill depth, where return geostrophic flow can be supported. Thus, the structure of the middepth, midlatitude thermocline is directly influenced by the geometry of the gap. A similar constraint evidently operates in the Southern Ocean.

1. The Gill and Bryan geometry

In a pioneering calculation, Gill and Bryan (1971) studied the effects of a circumpolar connection on numerical solutions of a primitive-equation ocean circulation model. The basin geometry was purposely kept simple: a rectangular box with vertical sidewalls, punctured by a gap near the southern end of the eastern and western boundaries, at which periodic boundary conditions were imposed to represent a circumpolar connection. The model circulation depended importantly on the existence of the gap and on whether it extended to the basin floor or only to middepth. The existence of the gap was offered as an explanation for the formation of Antarctic Intermediate Water, and the model circumpolar current appeared to be primarily thermal when the gap extended only to middepth.

The idealized geometric representation of the Antarctic region introduced by Gill and Bryan (1971) has formed the basis of several other numerical investigations using similar primitive equations (e.g., Cox 1989; Vallis 2000). However, despite the analytical treatment of related barotropic problems by Gill (1968), Kamenkovich (1962), and others, there has evidently been relatively little attention devoted to analytical models that include both thermal and wind stress forcing in this geometry.

The purpose of the present note is to describe a very simple analytical theory for steady, large-scale geostrophic circulation of a stratified fluid in the Gill and Bryan (1971) geometry, which illustrates some relations that arise in this geometry between the circumpolar current, the midlatitude thermocline, and the wind and thermal forcing in the vicinity of the circumpolar connection.

2. Model formulation

The geometry consists of a square basin of uniform depth on a southern-hemisphere β plane (Fig. 1). Horizonal distance is scaled by the basin width L, so the domain is $0 \le x \le 1$, $0 \le y \le 1$, where x and y are positive eastward and northward, respectively. Depth is scaled by the basin depth D, so the domain is $0 \le z \le 1$, where z is positive upward. The gap is located in $y_1 \le y \le y_2$, $z \ge H$ so that $z = H$ is the sill depth, and periodic boundary conditions are imposed at $x = 0$ and $x = 1$ in the gap.

The interior flow is described by ideal planetary geostrophic dynamics (geostrophy, hydrostatic balance, incompressibility, and material conservation of temperature in the Boussinesq approximation), with no salinity effects. Thermal diffusion is neglected, but convective adjustment is included to maintain static stability and plays a fundamental role in the solutions. Geostrophic boundary currents close the meridional transport; in

Corresponding author address: Dr. Roger M. Samelson, College of Oceanic and Atmospheric Sciences, Oregon State University, 104 Oceanography Admin. Bldg., Corvallis, OR 97331-5503.
E-mail: rsamelson@oce.orst.edu

© 1999 American Meteorological Society

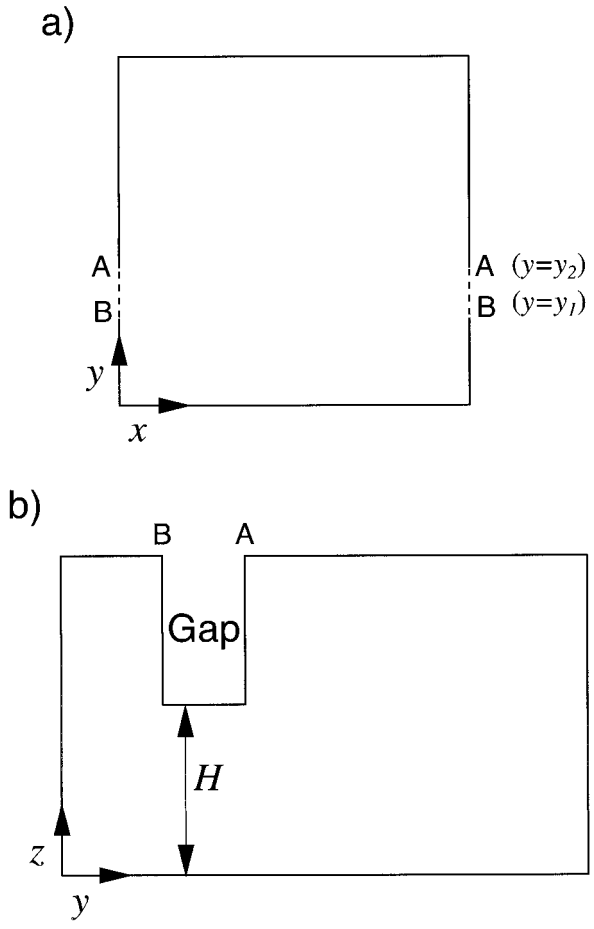

FIG. 1. Model geometry (schematic). (a) Plan view. The dashed lines A–B indicate the gap, where periodic boundary conditions are applied for $y_1 < y < y_2$, $z > H$. (b) Side view. The location of the gap and the height H of the sill are indicated, and the points A and B are labeled as in (a).

these, the cross-stream momentum balances are geostrophic, but the alongstream momentum balances are not specified.

Special forms of wind and thermal forcing are chosen for simplicity and to focus attention on the role of the circumpolar connection. The surface temperature $T_s = T(x, y, z = 1)$ is fixed to zero south of the gap, increases abruptly at the southern edge of the gap and then linearly across the gap to a maximum at the northern edge of the gap, and remains constant at this maximum value from the northern edge of the gap to the northern boundary of the basin:

$$T_s = \begin{cases} 0, & 0 \le y < y_1 \\ T_1 + \left(\dfrac{T_2 - T_1}{y_2 - y_1}\right)(y - y_1), & y_1 \le y < y_2 \\ T_2, & y \ge y_2. \end{cases} \tag{2.1}$$

The reason for the small but abrupt temperature increase from 0 to T_1 at the southern edge of the gap will be explained below.

The meridional surface Ekman transport v_E is given by

$$v_E = \begin{cases} \dfrac{1}{2}V_1\left[1 - \cos\left(\dfrac{\pi(y - y_s)}{\Delta y}\right)\right], & y_s \le y < y_1 \\ V_1, & y_1 \le y < y_m \\ \dfrac{1}{2}V_1\left[1 + \cos\left(\dfrac{\pi(y - y_m)}{\Delta y}\right)\right], & y_m \le y < y_n. \end{cases} \tag{2.2}$$

Here $y_s = y_1 - \Delta y$, $y_m = y_2 + \Delta y/2$, $y_n = y_m + \Delta y$, and $v_E = 0$ for $y < y_s$ and for $y > y_n$. Thus, the Ekman transport v_E is constant across a band of latitudes spanning the gap ($y_1 < y < y_2$) and extending north to $y = y_m$ (so the effective zonal wind stress across this band varies in concert with the Coriolis parameter) and falls smoothly to zero to the north and south. This Ekman transport results in an Ekman vertical velocity at the surface $z = 1$:

$$w_E = \frac{dv_E}{dy} = \begin{cases} W_1 \sin\left(\dfrac{\pi(y - y_s)}{\Delta y}\right), & y_s \le y < y_1 \\ 0, & y_1 \le y < y_m \\ -W_1 \sin\left(\dfrac{\pi(y - y_m)}{\Delta y}\right), & y_m \le y < y_n, \end{cases} \tag{2.3}$$

where $W_1 = \pi V_1/(2\Delta y)$.

The corresponding meridional profiles of T_s, v_E, and w_E are shown in Fig. 2 for the example with $y_s = 0$, $y_1 = 0.2$, $y_2 = 0.3$, $y_m = 0.4$, $y_n = 0.6$, $\Delta y = 0.2$, $H = 0.5$, $T_1 = 1.05$, $T_2 = 50$, $W_1 = 1$, and $f(y) = -1.125 + 0.5y$. Dimensional values may be computed using the scales $L = 5000$ km, $D = 5000$ m, $U_* = 10^{-3}$ m s^{-1}, $W_* = 10^{-6}$ m s^{-1}, and $T_* = 0.12$ K, for length, depth, horizontal velocity, vertical velocity, and temperature, respectively (see, e.g., Samelson and Vallis 1997). The values $f = -1$ and $\beta = \beta_* L/f_* = 0.5$ at $y = 0.25$ correspond to a latitude of 57°S in the center of the gap.

3. Model circulation

a. Southern gyre ($y < y_1$)

When the surface temperature T_s is given by (2.1), and no fluid with $T < 0$ is present, it follows that the fluid south of the gap ($y < y_1$) must have $T = 0$ everywhere, since $T_s = 0$ and any warmer fluid will be removed immediately by convective adjustment. Thus, the motion in the southern wind-forced region ($y_s < y < y_1$) is barotropic, and there is no motion south of the

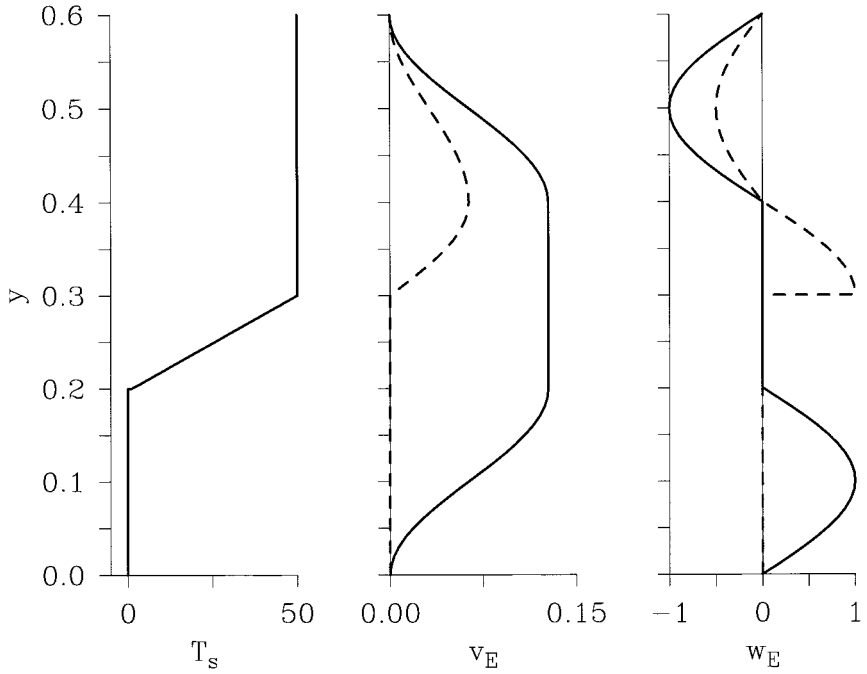

FIG. 2. Surface forcing. Surface temperature (left panel), meridional Ekman transport (center), and Ekman vertical velocity (right) vs y for $y_1 = 0.2$, $y_2 = 0.3$, $\Delta y = 0.2$, $T_1 = 1.05$, $T_2 = 50$, and $W_1 = 1$ (solid lines). With dimensional scales as in the text, the latitudinal distance shown is 3000 km, the total north–south temperature contrast is 6 K, the maximum Ekman transport (per unit zonal distance) is 0.64 $m^2\ s^{-1}$, and the maximum Ekman pumping velocity is 10^{-6} m s^{-1}. Dashed lines: Conceptual example of Ekman forcing discussed in section 4f.

wind-forced region ($y < y_s$). A zonal integral of the barotropic Sverdrup balance $\beta v = f w_E$ gives the surface pressure $p_s(x, y)$ in $y_s < y < y_1$,

$$p_s(x, y) = -W_1 \frac{f^2}{\beta}(1 - x) \sin\left(\frac{\pi(y - y_s)}{\Delta y}\right). \quad (3.1)$$

The western boundary current transport required to balance the Ekman and Sverdrup flow is

$$V_{bs} = -v_E - \frac{f}{\beta} w_E \quad (3.2)$$

for $y > y_s$ and zero for $y < y_s$. Figures 3 and 4 show p_s and V_{bs}, respectively, for forcing as above.

b. Northern gyre ($y > y_2$)

The sidewalls extend continuously around the basin up to the sill depth $z = H$. Consequently, meridional geostrophic flow can be supported continuously around the basin, and the entire basin will fill up to the sill depth with the coldest fluid available, except where the cold fluid is displaced by warm fluid that has been forced downward by the action of the wind. North of the gap ($y > y_2$), it is natural to make the traditional assumption that the geostrophic no-normal-flow condition may be applied directly to the interior flow along the eastern boundary so that isotherms along the eastern boundary must be flat. It follows that the fluid beneath the sill depth ($z < H$) must have $T = 0$ along the entire eastern boundary. Similarly, all the fluid beneath the sill depth in the stagnant region north of the wind forcing ($y > y_n$) must have $T = 0$.

Surface Ekman transport forces fluid northward across the gap, and the fixed surface thermal gradient implies that this fluid warms as it moves across the gap. North of the gap ($y > y_2$), the fluid pumped downward from the surface layer all has uniform temperature $T = T_2$. The geostrophic constraint prevents any southward return flow of this warm fluid across the gap above the sill depth. Along the eastern boundary, then, the warm ($T = T_2$) fluid will extend downward all the way to the sill depth $z = H$, where it first encounters opposition from cold ($T = 0$) fluid able to flow northward geostrophically. Accordingly, the fluid north of the gap divides into two layers, a lower layer that has $T = 0$ and is at rest and an upper layer of thickness $h(x, y)$ that has $T = T_2$ and is driven by Ekman pumping, with eastern boundary condition $h(1, y) = h_e = 1 - H$. The solution for the moving, upper layer north of the gap is

$$h(x, y) = (h_e^2 + D_0^2)^{1/2}, \quad (3.3)$$

where for $y_m < y < y_n$,

$$D_0^2 = \frac{2f^2}{T_2\beta} W_1(1 - x) \sin\left(\frac{\pi(y - y_2)}{\Delta y}\right), \quad (3.4)$$

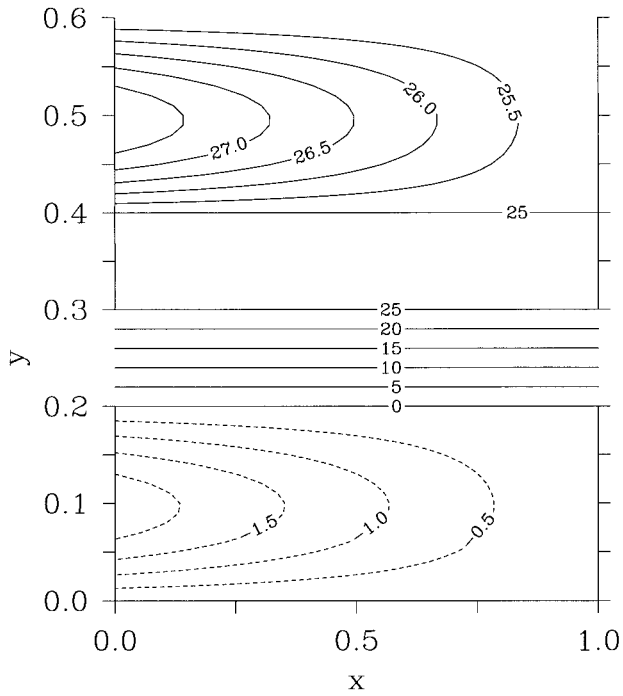

FIG. 3. Contours of surface pressure $p_s(x, y)$, with the forcing as in Fig. 2 and other parameters as in the text. The circulation is counterclockwise (anticyclonic) in the northern gyre and clockwise (cyclonic) in the southern gyre. The circumpolar zonal flow through the gap ($0.2 < y < 0.3$) is much stronger than the gyre circulations, and the contour increment increases accordingly from 0.5 in the gyres to 5 in the gap. For the circumpolar flow, with dimensional scales as in the text, the maximum dimensional surface speed is 26 cm s^{-1}, and the dimensional transport is 153×10^6 m^3 s^{-1}. Only the region $y < 0.6$ is shown, as there is no flow for $y > 0.6$.

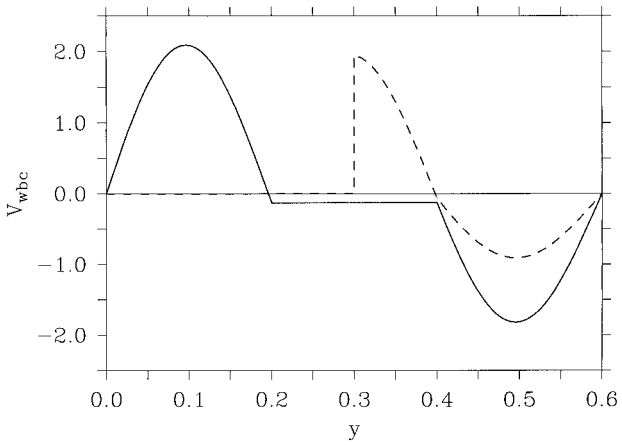

FIG. 4. Western boundary current transport (units of 25×10^6 m^3 s^{-1}, for dimensional scales as in the text) versus meridional distance y, for the solution in Fig. 3. Across the gap ($0.2 < y < 0.3$), the southward boundary current transport balances the northward Ekman transport $V_1 = 0.127$ (3.2×10^6 m^3 s^{-1}). The dashed lines indicate the boundary current transport for the Ekman forcing shown by dashed lines in Fig. 2.

and $D_0 = 0$ for $y_2 < y < y_m$ and for $y > y_n$. The surface pressure $p_s(x, y) = T_2 h(x, y)$, and the western boundary current transport is

$$V_{bn} = -v_E - \frac{f}{\beta} w_E \tag{3.5}$$

for $y_2 < y < y_n$ and zero for $y > y_n$. Figures 3 and 4 show p_s and V_{bn}, respectively, for forcing as above and in Fig. 2. The depth at $x = 0$ of the western boundary current in the northern gyre is also indicated in Fig. 5, which is discussed below.

c. Gap latitudes ($y_1 < y < y_2$)

When the warm fluid north of the gap reaches the sill depth, it may flow southward geostrophically across the gap to compensate the northward surface Ekman transport across the gap. However, as it does so, it will flow beneath colder surface fluid because of the fixed thermal gradient across the gap. To remove the resulting static instability, a convective adjustment process is imposed that mixes temperature vertically to neutral stability. The effect of this adjustment is that the water column at the sill assumes the local surface temperature throughout the depth range from the surface ($z = 1$) to the base of the boundary current ($z = d$) that flows southward along the sill.

Above the sill, then, the fluid in the gap has a simple structure: at each latitude, the surface temperature extends to the base of the gap: $T(0, y, z) = T_s(y)$ for $y_1 < y < y_2$, $z > H$. Associated with this meridional temperature gradient is a zonal geostrophic flow through the gap. A pure zonal geostrophic flow solves the in-

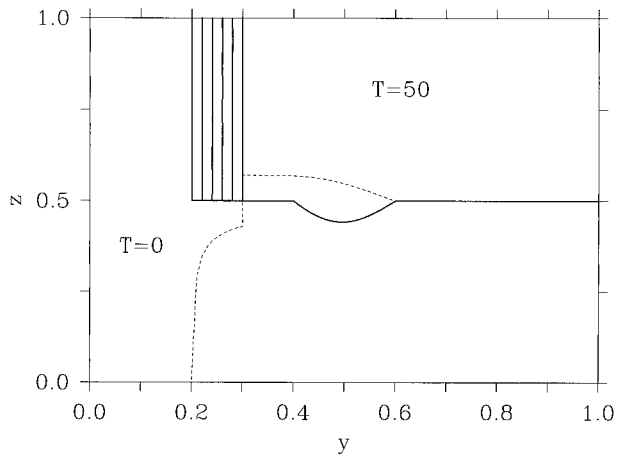

FIG. 5. Contours of temperature T versus depth z and meridional distance y on the eastern edge of the western boundary current ($x = 0$) for the solution in Fig. 3. The contours 0, 10, 20, 30, 40, and 50 are shown. The dashed line indicates the base of the western boundary current at the boundary. For $y > 0.6$, both layers are stagnant. The boundary current and interior are barotropic for $y < 0.2$. With dimensional scales as in the text, the total temperature contrast (50 units) is 6 K, the contour increment is 1.2 K, the basin depth is 5000 m, and the basin width is 5000 km.

terior equations exactly, so the temperature field in the gap may be extended zonally across the basin:

$$T(x, y, z) = T_s(y), \qquad y_1 < y < y_2, \qquad z > H. \quad (3.6)$$

Since the $T = 0$ abyssal interior fluid beneath the sill is stagnant, the interior pressure at the sill depth $z = H$ is uniform, and the hydrostatic and geostrophic relations may be used to construct the pressure p and zonal velocity u in the circumpolar current above the sill depth, yielding

$$p(y, z) = T_s(y)(z - H), \quad (3.7)$$

$$u(y, z) = -f^{-1}\left(\frac{T_2 - T_1}{y_2 - y_1}\right)(z - H) \quad (3.8)$$

for $y_1 < y < y_2$, $z > H$. The speed u and transport U,

$$U = \left(\frac{T_2 - T_1}{y_2 - y_1}\right)\frac{1}{2}(1 - H)^2\beta^{-1} \ln\frac{f(y_1)}{f(y_2)}, \quad (3.9)$$

of this circumpolar current depend only upon geometric and thermal parameters. Figure 3 shows the surface pressure $p_s(x, y) = p(y, 1)$ for this solution for forcing as above and in Fig. 2. For the dimensional scales given above, the dimensional values for the maximum current speed and total circumpolar current transport are 25 cm s^{-1} and 153 $\times$ 10^6 m^3 s^{-1}. The midbasin, meridional cross section of temperature in Fig. 5 illustrates that the strength of the middepth, midlatitude thermocline in this model depends directly on the meridional difference in surface temperature across the gap. Vallis (2000) shows a similar sketch of this dependence, on the basis of numerical calculations extending the approach of Gill and Bryan (1971) and Cox (1989).

At the southern edge of the gap ($y = y_1$), there is a small discontinuity in pressure above the sill depth ($z > H$) since $p = 0$ just south of $y = y_1$ and $p = T_1(z - H)$ just north of $y = y_1$. This discontinuity arises from the surface temperature jump at $y = y_1$, which was imposed for convenience, to make the southern gyre barotropic. Setting $T_1 = 0$ would remove the discontinuity, but would also remove the thermal gradient required to support the deep boundary current at the southern edge of the sill. Associated with the pressure jump is an infinitesimally thin zonal geostrophic jet at the southern edge of the gap with transport

$$U_1 = -\frac{T_1}{2f(y_1)}(1 - H)^2, \quad (3.10)$$

which has the value 3.2 $\times$ 10^6 m^3 s^{-1} for the dimensional scales given above. Since this transport is relatively small, the detailed dynamics of this jet are not pursued further here.

It is useful to give a concrete model of the southward-flowing geostrophic boundary current at the sill, which illustrates a possible thermal and velocity structure for the current. The thermal anomaly, relative to the stagnant $T = 0$ abyssal interior fluid beneath the sill, is assumed to be independent of depth within the boundary current and to decay exponentially offshore,

$$T_{bc} = T_s e^{-x/\varepsilon}, \qquad y_1 < y < y_2, \qquad d < z < H, \quad (3.11)$$

where d is the base of the moving fluid at the boundary, and ε is an arbitrary width scale for the boundary current. The hydrostatic relation may be integrated downward from the sill depth $z = H$, where $p = 0$, to determine the southward geostrophic flow in the boundary current, which increases with depth. A zonal integral across the boundary current gives the boundary current transport as a function of depth,

$$V_{bc}(y, z) = -f^{-1}T_s(z - H). \quad (3.12)$$

Since $f < 0$ and $z < H$ in the boundary current, V_{bc} is negative, as it must be to balance the northward Ekman transport. The total transport is

$$V_0 = \int_d^H V_{bc}\, dz = f^{-1}T_s\frac{1}{2}(H - d)^2. \quad (3.13)$$

Balancing V_0 against the northward Ekman transport across the gap V_1 determines d,

$$d(y) = H - \left|\frac{2fV_1}{T_s}\right|^{1/2}, \quad (3.14)$$

so the boundary current thickens and deepens southward, while slowing to maintain constant transport. The depth d of the moving fluid at the boundary is indicated in Fig. 5. The continuous horizontal thermal structure implies horizontal mixing of heat, in addition to the vertical mixing by convective adjustment adjacent to the sill where $T_{bc} = T_s$.

This boundary current model illustrates several points. First, if $T_s(y_1) = 0$, that is, if the surface temperature at the southern edge of the gap were equal to the temperature south of the gap, (3.14) would be singular at $y = y_1$, as there would be no thermal contrast available to support southward return flow in a geostrophic boundary current beneath the sill. Second, the boundary current model (when extended downward to $z < d$, using the hydrostatic relation) emphasizes that pressure gradients will be induced in the abyssal layer beneath the boundary current adjacent to the sill. These pressure gradients are neglected in the present model. This difficulty could be removed by introducing a small topographic slope along the eastern edge of the sill so that the boundary current extends to the bottom everywhere. Finally, the boundary current model illustrates that the southward geostrophic flow can occur as a downward deformation of isotherms along the eastern side of the sill, while the southward boundary current north of the gap naturally occurs as an upward deformation of isotherms since the level of no meridional motion is beneath the southward moving layer north of the gap but above the southward moving layer in the gap. The vertical motion implied in the boundary currents at the edges of the gap is discussed below.

4. Discussion

a. Nonlinear coupling

The structure of the solution depends critically on the southward-flowing boundary current beneath the sill of the gap. This current exists solely to balance the northward Ekman transport across the gap. In the absence of wind forcing there need be no such boundary current, and the temperature field in and north of the gap and above the sill depth is no longer uniquely constrained.

Thus, the surface Ekman transport across the gap, in the presence of surface thermal gradients across the gap (and with the restriction to zonally symmetric circumpolar flow through the gap), selects a particular circumpolar current structure from the many possible symmetric circumpolar flows that exist in the absence of wind forcing. However, as noted above, the structure and transport of the circumpolar current in this wind-forced state are determined entirely by thermal and geometric parameters and do not themselves depend on the strength of the wind forcing. This is a particularly clear and simple illustration of an intrinsically nonlinear coupling of wind-driven and thermal circulations.

b. Midlatitude thermocline

When there is a surface thermal gradient and Ekman transport across the gap, the depth to which warm fluid extends in the middepth, midlatitude thermocline is controlled in this model by the geometry of the gap. Also, there is a direct connection in the model between the surface temperature difference across the gap and the middepth, midlatitude stratification (Fig. 5) since the temperature difference across the base of the moving layer is equal to the imposed surface temperature difference across the gap latitudes. Vallis (2000) shows a similar sketch of this connection, based on analysis of numerical calculations extending the approach of Gill and Bryan (1971) and Cox (1989).

c. Deep boundary current

The model circulation requires large vertical motions in the western boundary current at the edges of the gap (Fig. 5). The fluid north of the gap moves southward in a single, homogeneous layer that extends from the surface to middepth. At the western boundary, the interface north of the gap lies 350 m (0.07 units) above the sill depth $z = H$, to support the net southward geostrophic transport, since the interface depth is $z = H$ at the eastern boundary. At the northern edge of the gap, the bottom of the southward moving column must drop from 350 m above $z = H$ to $z = d$, roughly 350 m below $z = H$. Simultaneously, the thickness of the southward-moving column must decrease precipitously from near $1 - H \approx 0.43$ (2150 m) to $H - d = |2fV_1/T_2|^{1/2} \approx 0.07$ (350 m). At the southern edge of the gap, the opposite must occur: the thin boundary current along the sill must spread vertically over the entire water column in order to match the barotropic flow south of the gap. The present analysis assumes that these vertical motions in the vicinity of the western boundary are possible and that substantial modifications of the interior circulation will not occur instead. The numerical solutions of Gill and Bryan (1971) show large vertical velocities along both the western and the eastern boundaries near the edges of the gap, an indication that large vertical motions can consistently occur in this region, at least in a numerical model, but it is uncertain whether these are related to the vertical motions in the present model.

d. Zonal momentum balance

In the vertically and zonally integrated zonal momentum balance at the gap latitudes, the effective wind stress is balanced by a pressure force on the basin walls that is associated with the geostrophic boundary current beneath the sill. If the wind stress in the gap is increased by increasing W_1, the pressure force will increase proportionally and the northern and southern gyres will intensify, but the thermal circumpolar circulation will be unaffected. Conversely, if the thermal gradient across the gap changes while the wind stress is held constant, the circumpolar flow will change, but the pressure force on the basin walls will not. There is no vertical transport of momentum through the circumpolar current itself and, since there are no waves in the model, there is no drag from wave processes in the latitude range of the gap. The zonal pressure force on the basin walls develops through the northern gyre from the Ekman flow that is forced northward across the gap. Since this zonal pressure force is associated with the meridional circulation and is essentially equivalent to the zonal pressure force that would support the return geostrophic flow in a closed basin, it seems inappropriate to consider it ''form drag,'' which classically describes a component of force directed parallel to the motion of the body or, if the body is at rest, parallel to the motion of the fluid past the body. From this point of view, it might be more appropriate to consider it a force of lift, rather than drag, since it is directed normal to the flow of the boundary current that is its proximate cause. However, this terminology could give the false impression that the force is upward.

e. Sverdrup-driven gap currents

In the model above, the zonal wind stress at the gap latitudes is taken up in the surface Ekman layer, and the circumpolar flow is a purely thermal current. Circulation may also be induced in the gap latitudes ($y_1 < y < y_2$) by southward Sverdrup flow across $y = y_2$, which is absent from the model above.

Provided that the wind stress at the gap latitudes will be balanced by Ekman transport as above, the Sverdrup-

driven component may be considered separately, with forcing restricted to the region north of the gap. The interesting case is when the impinging Sverdrup flow is confined above the sill depth. The simplest configuration in which this process can be represented is a reduced-gravity model, with a single moving layer of temperature $T = T_2$ and thickness h overlying a stagnant abyssal layer with temperature $T = 0$, and in which the mean value of h is chosen small enough so that the moving layer lies above the sill depth at the gap latitudes. The surface temperature is $T = T_2$ everywhere, and the wind stress (divided by a reference density) is

$$\tau^x = \begin{cases} 0, & y \le y_2 \\ f_2 W_2 (y - y_2), & y > y_2, \end{cases} \tag{4.1}$$

where $f_2 = f(y_2)$, W_2 is a constant, and $\tau^y = 0$ everywhere. For (4.1), $w_E(y = y_2) = W_2$, so the Sverdrup transport $V_S = (f_2/\beta)W_2$ across $y = y_2$ in the moving layer will be southward if $W_2 > 0$. Only motions induced by the forcing (4.1) are considered, and the fluid is otherwise at rest, with constant h.

Since there is no forcing for $y < y_2$, the fluid is at rest and h is constant for $y < y_2$, and the southward Sverdrup flow U_S across $y = y_2$,

$$U_S = -\int_0^1 V_S(x', y_2)\, dx' = -\frac{f_2}{\beta} W_2, \tag{4.2}$$

must be taken up in an infinitesimal internal boundary layer along $y = y_2$. The zonal jet associated with this internal boundary layer must reach the western boundary in order to allow the fluid to return northward in a western boundary current and close the circulation, as suggested by Stommel (1957), Wyrtki (1960), and Veronis (1973) for a related geometry.

It is necessary to determine in which direction this jet flows. Perhaps the simplest assumption is that, since there is no forcing in the gap latitudes, the zonally integrated zonal momentum of the flow in the jet must equal the zonally integrated zonal momentum of the flow immediately north of the northern edge of the gap latitudes, as the meridional displacement required to cross the edge of the gap latitudes and enter the jet is infinitesimal. Since the Sverdrup and geostrophic boundary current flow at $y = y_2$ are purely meridional and there is no zonal wind stress at $y = y_2$, this reasoning would evidently imply that the zonally integrated zonal momentum of the internal boundary layer jet must also be zero. This suggests that the jet will split, with half of the impinging Sverdrup transport U_S flowing directly westward to the western boundary and half flowing eastward through the gap.

To test this inference, it is useful to consider an explicit solution of a model that includes a simple representation of frictional effects. For the reduced-gravity model, a total transport streamfunction Ψ may be defined so that

$$hu = -\Psi_y, \qquad hv = \Psi_x, \tag{4.3}$$

where h is the thickness of the moving layer, (u, v) the depth-averaged velocities, and the wind stress τ will be treated as a body force ($\tau_z = \tau/h$). If frictional effects are parameterized by a simple linear drag law, $(\mathcal{F}^x, \mathcal{F}^y) = -r(u, v)$, then the resulting equation for Ψ is (Stommel 1948)

$$r(\Psi_{xx} + \Psi_{yy}) + \beta\Psi_x = \tau^y_x - \tau^x_y. \tag{4.4}$$

Solutions of (4.4) in a basin with a circumpolar connection have been obtained by Gill (1968). The present case differs slightly from the particular cases examined by Gill because the wind stress vanishes at the gap latitudes, but Gill's analytical results may still be used. For this purpose, it is convenient to extend the gap southward to $y = y_s$, so that there are no meridional boundaries south of $y = y_2$, and to place rigid zonal walls at $y = y_s = y_1 = 0$ and $y = y_n = 1$.

The vertically integrated no-normal-flow condition requires $\Psi_s = 0$ on the lateral boundaries, where s is a local tangent to the boundary. Along the eastern, northern, and western boundaries, Ψ must therefore be a constant, taken to be zero. Along the southern boundary, Ψ must also be constant, but this constant value Ψ_0 must be determined as part of the solution and gives the meridionally integrated, zonal circumpolar flow (at each longitude) through the gap. The vertically integrated zonal momentum balance,

$$-f\Psi_x = -T_2 h h_x + r\Psi_y + \tau^x, \tag{4.5}$$

may be integrated over the basin at the gap latitudes ($0 < x < 1$, $0 < y < y_2$), where $\tau^x = 0$ and the flow is zonally periodic, to obtain

$$\Psi_0 = \int_0^1 \Psi(x, y_2)\, dx. \tag{4.6}$$

Thus, the value of Ψ on the southern boundary is equal to the zonal average of Ψ along the northern edge of the gap latitudes.

In the limit $r \to 0$, the value of Ψ_0 for the wind forcing (4.1) may be calculated from Eq. (5.22) of Gill (1968). The result is

$$\Psi_0 = 0.5894 U_S \tag{4.7}$$

(where $0.5894 = \sigma_1$ in Gill's notation). Thus, in this model, friction slightly augments the eastward transport through the gap, relative to the value $\Psi_0 = U_S/2$ inferred above from inviscid arguments. Since there is no forcing at the gap latitudes, the zonally integrated zonal flow at the gap latitudes remains zero, as it must according to (4.6). From Eq. (5.28) and subsequent discussion in Gill (1968), the eastward transport in the boundary layer around the southern tip of the meridional boundary at $x = 0$, $y = y_2$ is $0.8240 U_S$ ($0.8240 = 2a_0$ in Gill's notation). The Sverdrup transport is equal to U_S north of the internal boundary layer, so a transport of $0.1760 U_S$ must enter the western boundary layer from the east, and a transport of $0.2346 U_S$ must pass westward

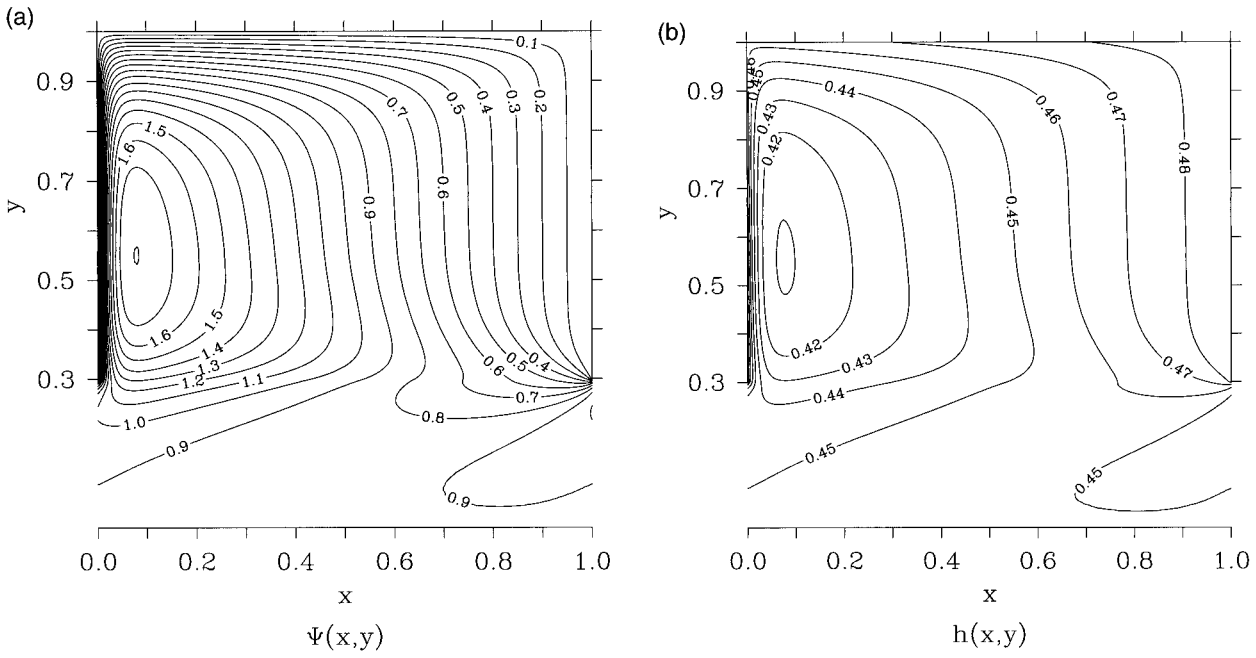

FIG. 6. Contours of (a) streamfunction Ψ and (b) layer thickness h for the solution of (4.4). Here $y_s = y_1 = 0$, so the gap extends from $y = 0$ to $y = y_2 = 0.3$. The surface temperature is uniform, and the wind forcing vanishes for $y < y_2$.

through the gap and then recirculate, turning northward and eastward to enter the western boundary current through the boundary layer at the southern tip of the meridional boundary.

To illustrate these results, a finite-difference numerical solution of (4.4) is shown in Fig. 6 for $y_s = 0$, $y_2 = 0.3$, $y_n = 1.0$, $W_2 = 1/f_2$, and $r = 0.01$. The grid resolution for this solution was $dx = dy = 0.005 = 0.25(r/\beta)$. For this solution, $\Psi_0 = 0.898$ and $U_S = 1/\beta = 2$, so $\Psi_0/U_S = 0.45$ and the eastward flow through the gap is roughly 20% less than the $r \to 0$ estimate (4.7). The zonally integrated zonal flow is zero in the gap latitudes, as it must be, according to (4.6). South of the northern edge of the gap ($y < y_2$), the flow between the $\Psi = 1.0$ and $\Psi = 1.3$ contours is westward. The $\Psi = 0.9$ contour indicates flow westward through the gap that recirculates eastward into the western boundary current. The flow between the $\Psi = 0$ and $\Psi = 0.7$ contours goes eastward through the gap and into the western boundary current. The corresponding upper-layer thickness h, with $h = 0.45$ specified along the southern boundary, is nearly flat across the gap latitudes and slopes upward to the west and downward to the east in the cyclonic gyre for $y > y_2$.

f. The Antarctic Circumpolar Current

The above results may be combined to suggest a conceptual model of the large-scale dynamics of the Antarctic Circumpolar Current (ACC). Since the Sverdrup and Ekman transport balances are linear, it is reasonable as a first approximation to simply superpose a thermal component, driven by the Ekman transport across the gap, and a Sverdrup component, driven by the divergence of Ekman transport just north of the gap indicated by the dashed lines in Fig. 2. Gradients in the thickness of the moving layer in the northern region and along the northern edge of the gap latitudes will support the Sverdrup component, essentially as in Fig. 6, except that now the interface will surface along the gap latitudes to support the thermal flow, as in Figs. 3 and 5. The eastward flow through the gap at $x = 1$ will consist of the thermal flow plus roughly half of the southward Sverdrup transport across $y = y_2$, while the zonally integrated zonal flow is due to the thermal flow alone and has no contribution from the Sverdrup component. A reversal of the zonal flow and the meridional thickness gradients is implied along meridional sections in the western part of the basin; this and the small cyclonic gyre that would form between y_2 and y_m might be loosely interpreted as suggesting a Sverdrup-driven northward shift of the circumpolar flow in the western part of the basin, which would seem more consistent with observations in the Southern Ocean.

While this conceptual model may be appealing in some respects, the present geometry, forcing, and dynamics are all extremely idealized, and inferences regarding the circulation of the Southern Ocean should be drawn only with appropriate caution. Two important uncertainties arise from the extreme idealization of the topography of the Southern Ocean and the neglect of mesoscale eddy effects. Flow driven by wind stress curl at the gap latitudes is also neglected in the model since

it cannot be supported by geostrophic Sverdrup transport above the sill depth.

The primary issue associated with the topography is whether the reentrant zonal channel properly represents the circumpolar connection through Drake Passage and its relation to the Antarctic Circumpolar Current. In general, the broad gap in the model likely constrains meridional motion at the gap latitudes too strongly. Stommel (1957) points out that, while Drake Passage itself is open to zonal flow down to at least 2000 m, most fixed latitude circles are blocked by topographic features at other longitudes [Stommel (1957, Fig. 25), note that panels (b) and (c) are reversed; see also Webb (1993, Fig. 9a)]. However, since unblocked latitude circles extending to depths of roughly 1500 m are found in narrow latitude bands within the latitudes spanned by Drake Passage, the reentrant zonal channel properly prevents meridional geostrophic flow above this depth; northward surface Ekman transport across the unblocked circles can return southward geostrophically only below the sill. Warren (1990) has argued that a deviation of only 1°–2° to the north or south of a latitude circle is sufficient to allow a similar circumpolar integration path through Drake Passage at depths down to at least 2000 m; while there are circumpolar passages deeper than 2000 m, Webb (1993) illustrates that a system of geostrophic zonal interior jets and meridional boundary currents can span the channel at any depth that is occluded by topographic barriers with sufficient meridional overlap.

The model thermal current and zonal jets, including especially the implied reversal of zonal currents in the western part of the basin, will almost certainly be unstable to mesoscale disturbances. These effects may be substantial: eddy heat fluxes may alter the thermal current, and eddy vorticity fluxes may disrupt the Sverdrup balance. Note that eddy momentum fluxes from baroclinic instabilities could also maintain the thermal current against friction; friction has been neglected in the thermal model, since the direction of the thermal current can be established independently, but is needed to obtain the constraint (4.6) in the Sverdrup-driven model.

Observations suggest that, to first order, the ACC transport at Drake Passage is comparable to the zonally integrated southward Sverdrup transport near 57°S, but there are substantial uncertainties in both the wind stress curl and the transport estimates (Baker 1982; Godfrey 1989; Chelton et al. 1990). Alternatively, the present results may also be compared briefly with results from numerical models, such as the FRAM primitive-equation Southern Ocean model, which had a horizontal grid resolution of roughly 25 km and included significant mesoscale eddy fluctuations (The FRAM Group 1991).

Saunders and Thompson (1993) verify explicitly that during the diagnostic phase of FRAM, the zonal wind stress in the FRAM ACC region is balanced near the surface by northward Ekman transport, and in vertical integral by bottom pressure forces associated with the meridional geostrophic return flow, and that the zonally integrated southward transport across 60°S is given by the Sverdrup balance. Wells and de Cuevas (1995) report that, on a nearly circumpolar path following mean streamlines westward from the west side of Drake Passage for longitudes from 70°W to 0°, and perhaps to 40°W, the Sverdrup transport balance dominated the integral of the depth-integrated vorticity equation in FRAM, and that there was little evidence of significant eddy contributions to the depth-integrated vorticity budget. These results are consistent with the assumption of surface Ekman and interior Sverdrup flow in the present model. The suggestion by Saunders and Thompson (1993), following Stommel (1957), that the FRAM ACC transport is set by the Sverdrup balance is at odds with the present results, which suggest that, in general, the southward Sverdrup flow across 60°S need not close eastward. Ivchenko et al. (1996) find that the vertically integrated alongstream momentum balance in FRAM is dominated by the balance of wind stress and bottom pressure force, consistent with the balance in the present model, but that friction and eddy stresses are not entirely negligible as assumed here.

5. Summary

A simple theory has been presented for steady geostrophic circulation of a stratified fluid in the Gill and Bryan (1971) geometry in which zonally reentrant flow is permitted through a gap in the sidewalls of a midlatitude basin. A circumpolar current arises in response to imposed surface thermal gradients and northward Ekman transport across the gap latitudes; its transport depends on the thermal gradients and the gap geometry, and not on the strength of the wind forcing. In contrast, zonal currents induced in a related reduced-gravity model by southward Sverdrup transport into the gap latitudes have zero zonally integrated zonal transport. When there is Ekman transport northward across the gap, the geostrophic constraint requires that the northern region fill with warm fluid until it reaches the sill depth where geostrophic return flow can be supported. Thus, the structure of the middepth, midlatitude thermocline is directly influenced by the geometry of the gap. A similar constraint evidently operates in the Southern Ocean.

Acknowledgments. I am grateful for conversations with G. Vallis, B. Warren, and R. de Szoeke, and for comments from two anonymous reviewers, which prompted the calculations in section 4e. This research was supported by the National Science Foundation, Division of Ocean Sciences (Grant OCE98-96184).

REFERENCES

Baker, D. J., Jr., 1982: A note on Sverdrup balance in the Southern Ocean. *J. Mar. Res.*, **40** (Suppl.), 21–26.

Chelton, D., A. Mestas-Nunez, and M. Freilich, 1990: Global wind

stress and Sverdrup circulation from the Seasat scatterometer. *J. Phys. Oceanogr.,* **20,** 1175–1205.

Cox, M., 1989: An idealized model of the world ocean. Part I: The global-scale water masses. *J. Phys. Oceanogr.,* **19,** 1730–1752.

The FRAM Group, 1991: Initial results from a fine resolution model of the Southern Ocean. *Eos, Trans. Amer. Geophys. Union,* **72,** 174–175.

Gill, A., 1968: A linear model of the Antarctic circumpolar current. *J. Fluid Mech.,* **32,** 465–488.

——, and K. Bryan, 1971: Effects of geometry on the circulation of a three-dimensional southern hemisphere ocean model. *Deep-Sea Res.,* **18,** 685–721.

Godfrey, J. S., 1989: A Sverdrup model of the depth-integrated flow for the world ocean allowing for island circulations. *Geophys. Astrophys. Fluid Dyn.,* **45,** 89–112.

Ivchenko, V., K. Richards, and D. Stevens, 1996: The dynamics of the Antarctic Circumpolar Current. *J. Phys. Oceanogr.,* **26,** 753–774.

Kamenkovich, V. M., 1962: K teorii Antarktichekogo Krugovogo Techeniya (On the theory of the Antarctic Circumpolar Current). *Trud. Inst. Okeanologii AN SSSR,* **56,** 241–293.

Samelson, R., and G. K. Vallis, 1997: Large-scale circulation with small diapycnal diffusion: the two-thermocline limit. *J. Mar. Res.,* **55,** 223–275.

Saunders, P., and S. Thompson, 1993: Transport, heat, and freshwater fluxes within a diagnostic numerical model (FRAM). *J. Phys. Oceanogr.,* **23,** 452–464.

Stommel, H., 1948: The westward intensification of wind-driven ocean currents. *Trans. Amer. Geophys. Union,* **29,** 202–206.

——, 1957: A survey of ocean current theory. *Deep-Sea Res.,* **4,** 149–184.

Vallis, G. K., 2000: Large-scale circulation and production of stratification: Effects of wind, geometry, and diffusion. *J. Phys. Oceanogr.,* in press.

Veronis, G., 1973: Model of world ocean circulation. Part I. *J. Mar. Res.,* **31,** 228–288.

Warren, B., 1990: Suppression of deep oxygen concentrations by Drake Passage. *Deep-Sea Res.,* **37,** 1899–1907.

Webb, D., 1993: A simple model of the effect of Kerguelen Plateau on the strength of the Antarctic Circumpolar Current. *Geophys. Astrophys. Fluid Dyn.,* **70,** 57–84.

Wells, N. C., and B. A. Cuevas, 1995: Depth-integrated vorticity budget of the Southern Ocean from a general circulation model. *J. Phys. Oceanogr.,* **25,** 2569–2582.

Wyrtki, K., 1960: The Antarctic Circumpolar Current and the Antarctic Polar Front. *Dtsch. Hydrogr. Z.,* **13,** 153–174.